

The Concept of Unidirectionally Coupled Nonlinear Circuits via a Memristor

CH.K. VOLOS^a, I.M. KYPRIANIDIS^b, I.N. STOUBOULOS^b, S.G. STAVRINIDES^b,
A.N. ANAGNOSTOPOULOS^b AND M. OZER^c

^aDepartment of Mathematics and Engineering Sciences, University of Military Education, Athens, GR 16673, Greece

^bPhysics Department, Aristotle University of Thessaloniki, Thessaloniki, GR 54124, Greece

^cDepartment of Physics, Istanbul Kultur University, Atakoy-Istanbul, Turkey

Confirmation of the existence of memristor by researchers at 2008 attracts much interest on this newly found circuit element. This is due to the fact that memristor opens up new functionalities in electronics and it has led to the interpretation of phenomena regarding not only electronics but also biological systems. In this work, we have studied the simulated dynamic behavior of two unidirectionally coupled nonlinear circuits via a memristor. This confirms the transition from chaotic desynchronization to complete chaotic synchronization through a regime of intermittent synchronization between the unidirectionally coupled circuits.

PACS: 05.45.Xt

1. Introduction

At the beginning of the 70's, Leon Chua reasoned that there should be a fourth fundamental electronic element, next to the three well known elements, namely the resistor (R), the capacitor (C) and the inductor (L). He was led to this assumption because a link between charge and flux was missing. Chua dubbed this missing link by introducing the memristor (short for memory resistor) [1] and created a crude example to demonstrate its key property i.e. that it becomes more or less resistive (less or more conductive) depending on the amount of charge that has flowed through it.

Until 2008, there has not been constructed such an electronic device, thus no real world confirmation existed. That year a physical model of a two-terminal device behaving as a memristor was announced in *Nature* [2]. Scientists at the Laboratories of Hewlett-Packard reported the realization of a new nanometer-scale electric switch, which "remembers" whether it is "on" or "off" after its power is turned off.

As a result, this discovery has attracted a great attention. This was reinforced by the fact that the features demonstrated by memristor could explain several phenomena in many nanoscale systems [3]. Memristors can also be used to design nonlinear oscillators by letting them to be the nonlinear device, for example, in Chua's circuit family [4–6].

Another point is that electronic circuits with memory circuit elements (memristors, memcapacitors and meminductors) can simulate processes typical of biological systems [7]. Nowadays, neuromorphic computing circuits are designed by borrowing principles of operation typical of the human (or animal) brain and therefore, due to their intrinsic analog capabilities they can potentially solve problems that are cumbersome (or outright intractable) by digital computation. Therefore, certain realizations

of memristors can be very useful in such circuits because of their intrinsic properties which mimic to some extent the behavior of biological synapses [8].

In this work, we have studied via computer simulations the dynamic behavior of two identical nonlinear circuits coupled via a memristor. The proposed memristor has a cubic nonlinear relation between flux (ϕ) and charge (q).

In the next sections the memristor and the coupled circuits are described, followed by the study of the dynamic behavior of the resulting dynamical system. Finally, conclusions remarks are presented in the last section.

2. The proposed memristor

The memristor is an electronic element which satisfies the relation between charge (q) and flux (ϕ), of Eq. (1). $W(q)$ is called memductance and relates memristor current (i_M) and voltage (v_M) through the relation of Eq. (2):

$$W(\phi) = \frac{dq(\phi)}{d\phi}, \quad (1)$$

$$i_M = W(\phi)v_M. \quad (2)$$

In the case of a linear element, W is a constant, and the memristor is identical to a resistor. However, in the case of memductance W being itself a function of a flux ϕ that is produced by a nonlinear circuit element, then no combination of the fundamental circuit elements, reproduces the same results as the memristor. Nowadays, many scientists consider memristor as a nonlinear circuit element with specific characteristics. For this reason various forms of memductances, such as cubic [4] or piecewise linear [5, 6], are proposed.

The proposed memristor is a flux-controlled memristor described by the function $W(\phi(t))$, where $q(\phi)$ in Eq. (3) is a smooth continuous cubic function of the form

$$q(\phi) = -k_1\phi + k_3\phi^3, \tag{3}$$

with $k_1, k_3 > 0$. As a result, in this case the memductance $W(\phi)$ is provided by the following expression:

$$W(\phi) = \frac{dq(\phi)}{d\phi} = -k_1 + k_3\phi^2. \tag{4}$$

3. The coupling scheme

In Fig. 1 two identical nonlinear circuits, which produce double scroll chaotic attractors [9], are unidirectionally coupled, via a memristor M . The buffer in the coupling branch isolates dynamics of the first circuit from the influence of the dynamics of the second circuit. The state equations, describing the normalized system, are as follows:

$$\begin{cases} \frac{dx_1}{d\tau} = y_1, \\ \frac{dy_1}{d\tau} = z_1 + \frac{R}{2}(k_1 + 3k_3w^2)(y_2 - y_1), \\ \frac{dz_1}{d\tau} = -\frac{x_1}{2} - \frac{y_1}{2} - \frac{z_1}{2} + \frac{R}{2R_x}f(x_1), \\ \frac{dx_2}{d\tau} = y_2, \\ \frac{dy_2}{d\tau} = z_2 + \frac{R}{2}(k_1 + 3k_3w^2)(y_1 - y_2), \\ \frac{dz_2}{d\tau} = -\frac{x_2}{2} - \frac{y_2}{2} - \frac{z_2}{2} + \frac{R}{2R_x}f(x_2), \\ \frac{dw}{d\tau} = \frac{RC}{2}(y_2 - y_1). \end{cases} \tag{5}$$

State variables $x_{1,2}$, $y_{1,2}$, and $z_{1,2}$, represent the voltages at the outputs of the operational amplifiers numbered as “1”, “2” and “3”, respectively (Fig. 1). The first three equations of system (5) describe the first of the two coupled identical double scroll circuits, while the other three describe the second one.

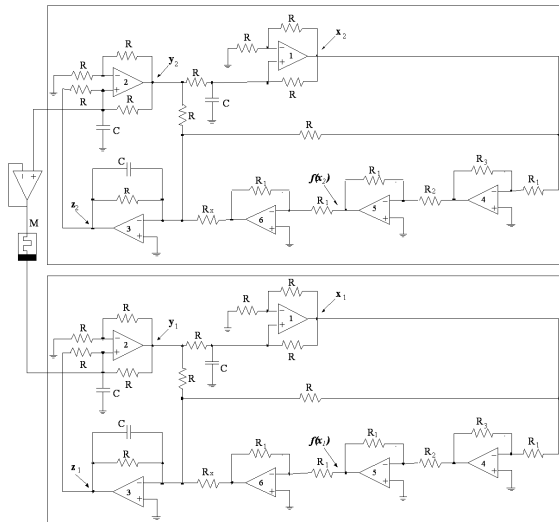


Fig. 1. The schematic of the double-scroll circuits, unidirectionally coupled via the memristor.

State variable w represents the magnetic flux (ϕ) of memristor M . The saturation functions $f(x_{1,2})$ used in

Eq. (5), are defined in Eq. (6), where $n = R_2/R_3$:

$$f(x_{1,2}) = \begin{cases} 1, & \text{if } x_{1,2} \geq n, \\ \frac{1}{n}x_{1,2}, & \text{if } -n \leq x_{1,2} < n, \\ -1, & \text{if } x_{1,2} < -n. \end{cases} \tag{6}$$

This implementation demonstrates an $i-v$ characteristic with two saturation plateaus at ± 1 , as well as an intermediate linear part with slope $1/n$.

The values of the circuit elements were: $R = 20.0 \text{ k}\Omega$, $R_1 = 1.0 \text{ k}\Omega$, $R_2 = 14.3 \text{ k}\Omega$, $R_3 = 20.4 \text{ k}\Omega$, $R_X = 12.5 \text{ k}\Omega$, and $C = 1.0 \text{ nF}$. All the operational amplifiers were of the type LF411. The voltages of the positive and negative power supplies were set to $\pm 15 \text{ V}$.

For this specific implementation, each circuit operated independently in a chaotic mode, demonstrating a double scroll chaotic attractor. This was further numerically confirmed by calculating the related Lyapunov exponents, which were found to possess the following values: $LE_1 = 0.13271$, $LE_2 = 0.00000$ and $LE_3 = -0.85410$ (at least one with positive value).

4. Dynamic behavior of the memristor coupled circuits

In this work, the dynamic behavior of the dynamical system described by Eq. (5) was studied numerically. We have chosen the factor $k_1 = 0.5 \times 10^{-4} \text{ C/Wb}$ of Eq. (4), while the other factor k_3 played the role of the bifurcation parameter. The system was numerically solved by employing a fourth order Runge–Kutta algorithm.

Next the bifurcation diagrams of $x_2 - x_1$ versus k_3 are shown. These diagrams were produced by increasing the factor k_3 , while the initial conditions of the system in each iteration remained the same. When the difference $x_2 - x_1$ becomes equal to zero, this means that the two coupled circuits are in chaotic synchronization.

In detail, two bifurcation diagrams of $x_2 - x_1$ versus k_3 , for two different sets of initial conditions, are shown in Fig. 2. In general, the morphology in both bifurcation diagrams of Fig. 2 is the same, with a difference at the width of the chaotic desynchronization region. As one can observe every single circuit remains in a chaotic state for a wide range of values of k_3 . Then the system, in both cases, turns from chaotic desynchronization to chaotic synchronization. It should be mentioned that the coupled system was at the saturation region for low values of factor k_3 . This is the reason why the two bifurcation diagrams of Fig. 2 begin at the value of $k_3 = 1 \times 10^4 \text{ C/Wb}^3$.

In Fig. 3 phase portraits of x_2 versus x_1 , for various values of the parameter k_3 in the case of the first bifurcation diagram in Fig. 2a, are shown. As we can see in Fig. 3a the system demonstrates an expanded range of chaotic desynchronization for low values of k_3 ($1 \times 10^4 \text{ C/Wb}^3 \leq k_3 < 3.88 \times 10^4 \text{ C/Wb}^3$). Then the system passes to a more limited chaotic desynchronization region for $3.88 \times 10^4 \text{ C/Wb}^3 \leq k_3 < 5.58 \times 10^4 \text{ C/Wb}^3$ (Fig. 3b).

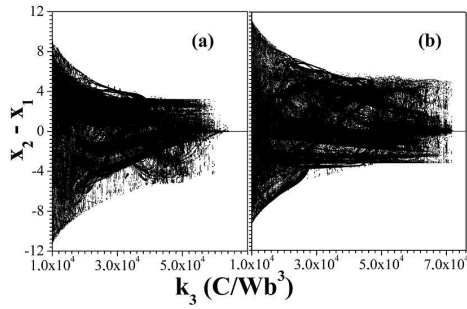


Fig. 2. Bifurcation diagrams ($x_2 - x_1$ vs. k_3), with $k_1 = 0.5 \times 10^{-4}$ C/Wb and initial values: (a) $(x_1, y_1, z_1, x_2, y_2, z_2, w) = (2, 1, 0.1, 0.8, 1.5, 0.05, 0.00001)$ and (b) $(x_1, y_1, z_1, x_2, y_2, z_2, w) = (-1, 0.5, 0.08, 1, -1.5, -0.03, 0)$.

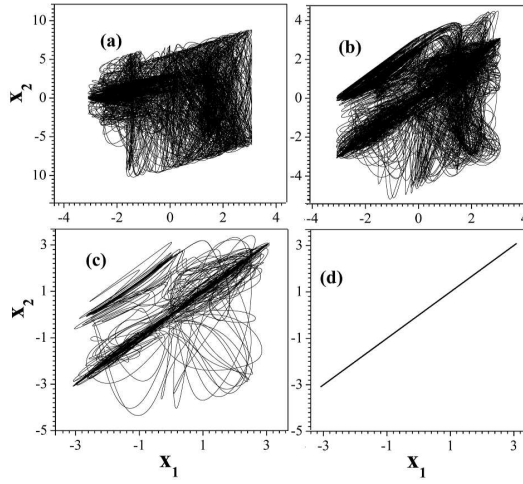


Fig. 3. Phase plot (x_2 vs. x_1) with $k_1 = 0.5 \times 10^{-4}$ C/Wb and for the set of initial values of Fig. 2a: (a) $k_3 = 1.5 \times 10^4$ C/Wb³ — expanded chaotic desynchronization, (b) $k_3 = 5 \times 10^4$ C/Wb³ — chaotic desynchronization, (c) $k_3 = 5.7 \times 10^4$ C/Wb³ — incomplete synchronization and (d) $k_3 = 9 \times 10^4$ C/Wb³ — chaotic synchronization.

In the region between desynchronization to synchronization (5.58×10^4 C/Wb³ $\leq k_3 < 6.4 \times 10^4$ C/Wb³), it is shown that an intermediate regime of incomplete synchronization emerges. The synchronization phase portraits consist of trajectories spending most of the time on the diagonal, only temporarily escaping from it (Fig. 3c). These escapes correspond to the bursts in the difference signal. The difference signal is almost zero for long time spaces, bursting only occasionally at significantly non-zero values. These bursts become of shorter duration and appear more infrequently, with increasing values of k_3 . This is confirmed in Fig. 4, where the corresponding time-series of signal $[x_2(t) - x_1(t)]$, for $k_3 = 5.7 \times 10^4$ C/Wb³ is shown. Finally, the system, for $k_3 \geq 6.4 \times 10^4$ C/Wb³, remains always in complete chaotic synchronization state (Fig. 3d).

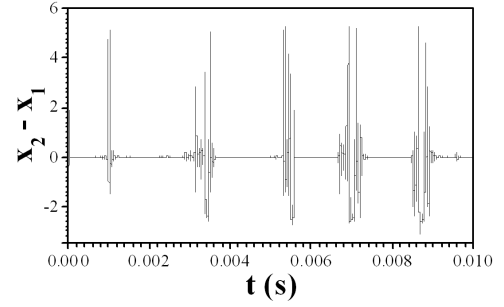


Fig. 4. Timeseries of signal $[x_2(t) - x_1(t)]$, in the case of intermittent synchronization of Fig. 3c.

5. Conclusion

In this report we have studied the unidirectionally coupling scheme between two identical nonlinear circuits via a memristor. The fact that memristors mimic the behavior of biological synapses makes the conclusions of this approach very interesting. Also, the coupling system via the memristor shows similar but more interesting behavior in relation to that observed in the coupling between the same circuits via a linear resistor [10]. In general, as the coupling parameter k_3 is increased, the system undergoes a transition from chaotic desynchronization to complete chaotic synchronization through a regime of intermittent synchronization.

References

- [1] L.O. Chua, *IEEE Trans. Circuit Theory* **CT-18**, 507 (1971).
- [2] D. Strukov, G. Snider, G. Stewart, R. Williams, *Nature* **453**, 80 (2008).
- [3] Y.V. Pershin, M. Di Ventra, *Phys. Rev. B, Condens. Matter* **78**, 113309 (2008).
- [4] I.M. Kyprianidis, Ch.K. Volos, I.N. Stouboulos, *AIP Conf. Proc.* **1203**, 626 (2010).
- [5] M. Itoh, L.O. Chua, *Int. J. Bifurcation Chaos* **18**, 3183 (2008).
- [6] B. Muthuswamy, *Int. J. Bifurcation Chaos* **20**, 1335 (2010).
- [7] Y.V. Pershin, S. La Fontaine, M. Di Ventra, *Phys. Rev. E* **80**, 021926 (2009).
- [8] S.H. Jo, T. Chang, I. Ebong, B.B. Bhadviya, P. Mazumder, W. Lu, *Nano Lett.* **10**, 1297 (2010).
- [9] Ch.K. Volos, I.M. Kyprianidis, I.N. Stouboulos, A.N. Anagnostopoulos, *J. Appl. Function. Anal.* **4**, 703 (2009).
- [10] Ch.K. Volos, I.M. Kyprianidis, S.G. Stavrinos, I.N. Stouboulos, A.N. Anagnostopoulos, *J. Eng. Sci. Technol. Rev.* **3**, 41 (2010).